

## Hydrodynamic efficiency of illumination by ion beams

By M. M. BASKO

Institute of Theoretical and Experimental Physics, B. Chermushkinskaya, 25, Moscow 117259

(Received 2 August 1989)

The hydrodynamic efficiency of conversion of the energy of fast charged particles into the kinetic energy of the bulk motion of plane-parallel shells is investigated in the framework of two simple models—one based on the stepwise density profile and the other employing a self-similar solution. The analytical estimates obtained are substantiated with 1D hydrodynamic calculations. In case of spherical shells, the three key dimensionless parameters determining the values of the hydrodynamic efficiency are pointed out; the dependence of the hydrodynamic efficiency on these parameters has been explored numerically. The effects of a nonuniform energy deposition (increasing by the end of the fast particle ranges) and of a nonuniform absorber composition are also discussed.

### 1. Introduction

The target energy gains in the inertial confinement fusion (ICF) to a large extent are determined by the initial stage of the implosion, at which the driver energy is being transformed into the kinetic energy of imploding shells (Duderstadt & Moses 1982). The hydrodynamic efficiency (HE) serves as a quantitative measure of the effectiveness of such an energy conversion. A number of publications exist that deal with the theory of HE for laser-driven targets (Afanas'ev *et al.* 1975, 1982; Max *et al.* 1983). This paper discusses the HE of plane-parallel and spherical shells illuminated by fast charged particles, with a special emphasis on the heavy ion beams.

This paper differs from earlier publications on laser targets and from the paper by Afanas'ev *et al.* (1981), in which irradiation by charged particles has also been considered, in that the steady-state approximation is discarded as nonrelevant. As shown below, nonsteady estimates of the HE may differ from the steady-state ones by as much as 100%. At the same time, nonsteady hydrodynamics is difficult to approximate with analytical models and one is forced to resort mostly to computer simulations.

### 2. Basic assumptions

From the point of view of the HE theory, a single-shell target can be treated as consisting of two layers—an absorber heated by fast ions and a pusher (payload), which is accelerated by the pressure in the absorber and pushes the rarefied gas ahead of itself (see figure 1). However, because the mass ranges of fast ions vary (and, in general, nonmonotonously; see Basko 1984) with the varying temperature and density in the absorber, the boundary between the pusher and the absorber even in the plane-parallel geometry cannot be clearly defined. But in practice, variations in the mass range of heavy ions are not large ( $\pm 10$ –15%) and, to get rid of this sort of an uncertainty, it is assumed that the mass coordinate of the pusher-absorber interface does not change with time (even in spherical geometry).

The other simplifying assumption that is employed in sections 3 and 4 infers that the absorber has uniform initial composition and density distributions and that the beam energy

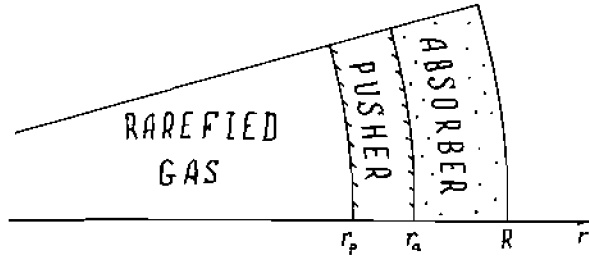


FIGURE 1. Structure of a shell illuminated by fast ion beams.

is being released uniformly over the absorber mass at a constant rate within the time interval  $0 < t < t_{in}$  (a box pulse). The effects of a nonuniform energy deposition (increasing to the end of the range; Ahlen 1980) and of a nonuniform absorber composition are discussed in section 5. Here, it should be noted only that the increase in the stopping powers of dense partially ionized plasmas by the end of the range of heavy ions is not particularly high (typically by a factor of  $\sim 1.5$ – $2$ ; see Basko & Sokolovskii 1982); in addition, its effect on the values of the HE is diminished by the range variations shifting the location of the heating-rate peak with time. After one accounts for the fact that the errors introduced into the HE values by the above two assumptions partially cancel one another, it turns out that the values of the HE as calculated in sections 3 and 4 quite adequately reproduce those achieved in code simulations of ICF targets driven by heavy ion beams—at least to the accuracy with which under such circumstances the quantity of the HE can be defined at all.

### 3. Planar shells

In the plane-parallel limit (see figure 1)

$$l_a \equiv R - r_a \ll R, \quad l_p \equiv r_a - r_p \ll R \quad (1)$$

it would be only natural to define the HE as

$$\eta_{pl} = \lim_{t \rightarrow \infty} \frac{E_{pk}}{E_{in}}, \quad (2)$$

where  $E_{pk}$  is the pusher kinetic energy and  $E_{in}$  is the total energy released in the absorber; the entire pusher mass is assumed to move with negative velocities. The HE—a dimensionless quantity—must be a function of dimensionless target parameters. The “external” dimensional parameters of a two-layer shell can be combined into the following independent dimensionless combinations

$$\mu = \frac{M_p}{M_a}, \quad \omega_0 = \frac{\rho_{0p}}{\rho_{0a}} = \frac{l_a}{l_p} \mu, \quad \tau_a = \frac{t_{in}}{l_a} \sqrt{\frac{E_{in}}{M_a}}. \quad (3)$$

Here,  $M_a$ ,  $M_p$ ,  $\rho_{0a}$ ,  $\rho_{0p}$  are the masses and initial densities of the absorber and the pusher. In addition to these “external” ones, a number of “internal” dimensionless shell parameters can be pointed out, which characterize the pusher and absorber equations of state, the role of the electron conductivity, the radiative losses, etc. Here it is argued that under the typical conditions of the ion-beam driven ICF of all the above-mentioned dimensionless parameters, the key role for the values of the plane-parallel HE belongs to the ratio  $\mu = M_p/M_a$ ;

in other words, for all practical purposes one can consider the plane-parallel HE to be a function of the pusher/absorber mass ratio only,

$$\eta_{pl} = \eta_{pl}(\mu). \quad (4)$$

It should be noted here that the initial pusher/absorber density ratio  $\omega_0$  is always assumed to be  $\geq 1$ . In the opposite limit  $\rho_{op} \ll \rho_{oa}$ , the parameter  $\omega_0$  would also become important. This latter limit, however, appears to be of much less practical interest; on the other hand, the very notion of HE in this limit becomes irrelevant because with  $\omega_0 \ll 1$ ,  $\mu \sim 1$  a substantial fraction of the pusher mass acquires positive velocities at  $t \gg t_{in}$ .

### 3.1. A stepwise-density-profile approximation

A relatively simple estimate of the plane-parallel HE can be derived if one assumes the velocity and density profiles

$$u(t, r) = U \frac{r - r_0}{R - r_0}, \quad (5)$$

$$\rho(t, r) = \begin{cases} \rho_a, & r_a < r < R, \\ \omega \rho_a, & r_p < r < r_a, \end{cases} \quad (6)$$

and applies the laws of mass, momentum and energy conservation to the shell as a whole. The quantities  $U$ ,  $\rho_a$ ,  $R$ ,  $r_a$ , and  $r_p$  are time-dependent, and  $\omega$  is a constant. The distributions (5) and (6) are mutually consistent in the sense that a linear velocity profile (5) preserves the density distribution (6). The mass and momentum conservation equations

$$\int_{r_p}^{r_a} \rho dr = \mu \int_{r_a}^R \rho dr, \quad \int_{r_p}^R \rho u dr = 0 \quad (7)$$

result in

$$\omega(r_a - r_p) = \mu(R - r_a), \quad (8)$$

$$R + r_a - 2r_0 + \mu(r_a + r_p - 2r_0) = 0, \quad (9)$$

which imply that

$$\frac{r_0 - r_a}{R - r_0} = \frac{1 - \mu^2/\omega}{1 + 2\mu + \mu^2/\omega}. \quad (10)$$

Under the condition

$$\mu < \sqrt{\omega} \quad (11)$$

the pusher-absorber interface  $r = r_a$  and the entire pusher move in the negative direction. It is assumed below that the allowed values of  $\mu$  satisfy condition (11).

In the limit

$$t \gg \max\{t_{in}, l_a \sqrt{M_a/E_{in}}\}, \quad (12)$$

conforming to definition (2) the internal energies of both the pusher and absorber can be ignored, and

$$\eta_{pl} = \left(1 + \frac{E_{ak}}{E_{pk}}\right)^{-1}, \quad (13)$$

where

$$E_{ak} = \frac{1}{2} \int_{r_0}^R \rho u^2 dr, \quad E_{pk} = \frac{1}{2} \int_{r_p}^{r_0} \rho u^2 dr. \tag{14}$$

From (5), (6), (8), (10), (13), and (14) we get

$$\eta_{pl} = \left\{ 1 + \frac{1}{\mu} \frac{1 + 2\mu + \mu^2 \left[ 4 + 3 \frac{\mu}{\omega} \left( 2 + \frac{\mu}{\omega} \right) \right]}{3 + \frac{\mu}{\omega} \left[ 6 + \frac{\mu}{\omega} (4 + 2\mu + \mu^2) \right]} \right\}^{-1}. \tag{15}$$

As shown below, of most practical interest is the limit  $\omega \rightarrow \infty$  when equation (15) takes a simple form

$$\eta_{pl} = \left( \frac{5}{3} + \frac{1}{3\mu} + \frac{4}{3} \mu \right)^{-1}. \tag{16}$$

First, note that the limit  $\tau_a \gg 1$  (see equation (3)) of an infinitely slow energy release just corresponds to  $\omega = \infty$ , because all the pusher elements in this limit move with one and the same speed. In the opposite limit of an instantaneous energy input, when  $\tau_0 = 0$ , the value of  $\omega$  can be estimated from the solution for a strong discontinuity decay used in the theory of shock tubes (Zel'dovich & Raizer 1966). Assuming that the pusher and absorber consist of an ideal gas with the same adiabatic index  $\gamma$  and the same initial density ( $\omega_0 = 1$ ), from the formulae in (Zel'dovich & Raizer 1966) we obtain the following values for  $\omega(\gamma)$ :

$$\omega\left(\frac{7}{5}\right) = 10.43, \quad \omega\left(\frac{5}{3}\right) = 6.50, \quad \omega(2) = 4.57. \tag{17}$$

If  $\omega_0 > 1$ , actual values of  $\omega(\gamma)$  will be even higher. Summing up, we conclude that the values  $\omega \geq 6$  are of practical interest and the dependence of  $\eta_{pl}$  on  $\omega$  can be ignored (especially when  $\mu \leq 0.3$ , see figure 2), and a simple expression (16) can be adopted. These same

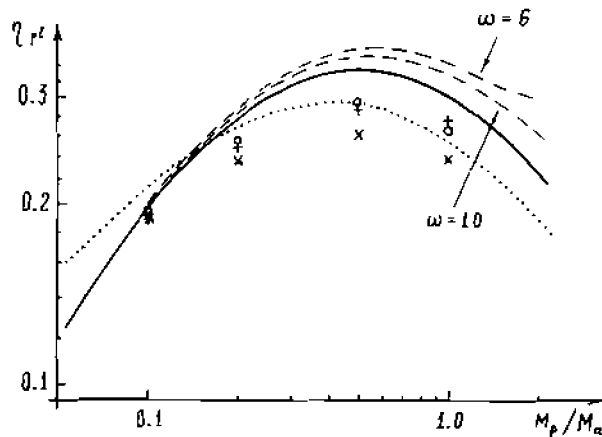


FIGURE 2. Hydrodynamic efficiency  $\eta_{pl}$  of planar shells as a function of the pusher/absorber mass ratio. Solid line, the plot of equation (16); broken lines, the plots of equation (15) for  $\omega = 6$  and  $\omega = 10$ ; dotted line, the plot of equation (29). Straight crosses, oblique crosses, and open circles, the values of  $\eta$  from the 1st, 3rd, and 5th columns in table 2.

TABLE 1.

$\omega$	1	4	6	10	$\infty$
$\mu_{\max}$	1.0	0.61	0.57	0.54	0.5
$\eta_{pl,\max}$	0.500	0.377	0.362	0.350	0.333

considerations prove also that the plane-parallel HE only weakly depends on the other two "external" dimensionless parameters from equation (3) —  $\tau_a$  and  $\omega_0$  (for  $\omega_0 \geq 1$ ). The maximum values of the function  $\eta_{pl}(\mu, \omega)$  for some  $\omega$  are given in table 1.

### 3.2. Self-similar solution

Earlier, to evaluate the HE of planar shells, Afanas'ev *et al.* (1981) employed a self-similar solution from Nemchinov (1961) describing the steady-state uniform heating of an absorber that accelerates an infinitely thin ( $r_a = r_p$ ) pusher with a finite surface mass density. For a box pulse of duration  $t_{in}$  this solution is valid within the time interval  $0 < t < t_{in}$ . However, as justly mentioned by Nemchinov (1961), the problem remains self-similar for later times  $t > t_{in}$  as well, after the energy input is switched off. In this latter case it belongs to the class of adiabatic flows with linear velocity profiles described by Sedov (1981). As a result, the complete nonsteady self-similar solution for an absorber with adiabatic index  $\gamma$  is as follows:

$$u(t, r) = \begin{cases} q^{1/2} t^{1/2} \frac{3}{2} \xi = \frac{3}{2} \frac{r - r_0}{t}, & 0 < t < t_{in}, \\ y \left[ \frac{3}{4(\gamma - 1)} (3\gamma - 1 - 2y^{\gamma-1}) \right]^{1/2} \frac{r - r_0}{t_{in}}, & t_{in} < t; \end{cases} \quad (18)$$

$$\rho(t, r) = \begin{cases} m_a q^{-1/2} t^{-3/2} D, & 0 < t < t_{in}, \\ m_a q^{-1/2} t_{in}^{-3/2} y D, & t_{in} < t; \end{cases} \quad (19)$$

$$P(t, r) = \begin{cases} m_a q^{1/2} t^{-1/2} \frac{2(\gamma - 1)}{3\gamma - 1} D, & 0 < t < t_{in}, \\ m_a q^{1/2} t_{in}^{-1/2} \frac{2(\gamma - 1)}{3\gamma - 1} y^\gamma D, & t_{in} < t. \end{cases} \quad (20)$$

Here  $r = r_0$  is the motionless center of mass,  $q$  [erg · g<sup>-1</sup> · s<sup>-1</sup>] is the heating rate in the absorber at  $0 < t < t_{in}$ , and  $m_a = \int_{r_a}^R \rho dr$  is the absorber surface mass density. The functions  $y = y(\tau)$  and  $D = D(\xi)$  satisfy the differential equations

$$\frac{dy}{d\tau} + y^2 \left[ \frac{3}{4(\gamma - 1)} (3\gamma - 1 - 2y^{\gamma-1}) \right]^{1/2} = 0, \quad (21)$$

$$\frac{dD}{d\xi} + \frac{3(3\gamma - 1)}{8(\gamma - 1)} \xi D = 0, \quad (22)$$

where

$$\tau = \frac{t}{t_{in}} \geq 1, \quad (23)$$

$$\xi = \begin{cases} q^{-1/2} t^{-3/2} (r - r_0), & 0 < t < t_{in}, \\ q^{-1/2} t_{in}^{-3/2} (r - r_0) y, & t_{in} < t. \end{cases}$$

The boundary condition for  $y(\tau)$  is

$$y(1) = 1; \quad (24)$$

the normalization of  $D(\xi)$  and the self-similar coordinate of the pusher  $\xi_p$  are determined by the conditions of the absorber mass normalization,

$$\int_{\xi_p}^{\infty} D(\xi) d\xi = 1, \quad (25)$$

and of the shell momentum conservation

$$\mu \xi_p + \int_{\xi_p}^{\infty} \xi D(\xi) d\xi = 0. \quad (26)$$

The steady-state HE calculated for  $t < t_{in}$  is

$$\eta_{pl,st} = \frac{\frac{1}{2} \mu m_a (q^{1/2} t^{1/2} \frac{3}{2} \xi_p)^2}{m_a q t} = \frac{6(\gamma - 1)}{3\gamma - 1} \mu g^2, \quad (27)$$

where the function  $g = g(\mu)$  is implicitly defined by

$$\sqrt{\pi} \mu g \exp(g^2) [1 + \operatorname{erf}(g)] = 1; \quad (28)$$

here  $\operatorname{erf}(x) = 2/\sqrt{\pi} \int_0^x e^{-t^2} dt$ . The complete (nonsteady) HE, attained in the limit  $t \gg t_{in}$ , is

$$\eta_{pl} = \frac{1}{2} \mu m_a \left[ \frac{3(3\gamma - 1)}{4(\gamma - 1)} q t_{in} \xi_p^2 \right] (m_a q t_{in})^{-1} = 2\mu g^2. \quad (29)$$

One immediately sees that the nonsteady HE (29) significantly (by factor of 2 for  $\gamma = 5/3$ ) exceeds the steady-state estimate (27) used by Afanas'ev *et al.* (1981). The reason for that is simple: the internal energy accumulated by the absorber during the ion-beam illumination phase keeps pushing the payload after the pulse had been stopped. Note also that the full HE (29) is independent of  $\gamma$ . The latter may be considered a confirmation of the weak dependence of the nonsteady HE on details of the pusher and absorber equations of state—as declared above.

### 3.3. Numerical results

To test the above analytical estimates of the plane-parallel HE, three series of 1D hydrodynamic calculations have been performed. In each series a set of four values of  $\mu = 0.1, 0.2, 0.5, 1.0$  has been probed. The initial conditions and the energy-input parameters have been chosen as follows.

1st series: absorber and pusher made of gold; the rarefied gas at  $0 < r < r_p$ —deuterium;

$$r_p = 9.99 \text{ mm}, 9.98 \text{ mm}, 9.95 \text{ mm}, 9.9 \text{ mm};$$

$$r_a = 10 \text{ mm}; R = 10.1 \text{ mm}; \rho_{0a} = \rho_{0p} = 19.5 \text{ g/cc};$$

$$E_{in}/M_a = 10 \text{ MJ/g}; t_{in} = 0.1 \text{ ns}; \omega_0 = 1; \tau_a = 0.1.$$

2nd series: absorber and pusher made of gold; the rarefied gas—deuterium;

$$r_p = 99.99 \text{ mm}, 99.98 \text{ mm}, 99.95 \text{ mm}, 99.9 \text{ mm};$$

$$r_a = 100 \text{ mm}; R = 100.1 \text{ mm}; \rho_{0a} = \rho_{0p} = 19.5 \text{ g/cc};$$

$$E_{in}/M_a = 10 \text{ MJ/g}; t_{in} = 10 \text{ ns}; \omega_0 = 1; \tau_a = 10.$$

3rd series: pusher made of gold, absorber made of beryllium; the rarefied gas—deuterium;

$$r_p = 99.99 \text{ mm}, 99.98 \text{ mm}, 99.95 \text{ mm}, 99.9 \text{ mm};$$

$$r_a = 100 \text{ mm}; R = 101 \text{ mm}; \rho_{0p} = 19.5 \text{ g/cc};$$

$$\rho_{0a} = 1.95 \text{ g/cc}; E_{in}/M_a = 10 \text{ MJ/g};$$

$$t_{in} = 0.1 \text{ ns}; \omega_0 = 10; \tau_a = 0.01.$$

The total mass of deuterium in all runs was fixed at 1% of the pusher mass. Realistic equations of state from Basko (1985) have been used for all elements. The electron and radiative heat conductions were also accounted for.

For the hydrodynamic efficiency the expression

$$\eta = \frac{E_p + E_c}{E_{in}} \quad (30)$$

was used, where  $E_p$  and  $E_c$  are the total energy values of the pusher and deuterium by the time when the coordinate of the inner pusher edge arrives at 1/10 of its initial value (by this time the absorber expands at least by a factor of 100). Table 2, in which thus obtained values of  $\eta$  are given, convincingly illustrates the weak dependence of the plane-parallel HE on parameters  $\omega_0$  and  $\tau_a$  (for  $\omega_0 \geq 1$ ) as well as on parameters of the equation of state.

When comparing the values of  $\eta$  from table 2 with analytical estimates (16) and (29), one must keep in mind that the limit  $t = \infty$ —in which equations (16) and (29) have been obtained—cannot be reached in numerical simulations. A good idea of the limiting HE in numerical runs can be obtained by means of the correction factor

$$\eta_{pl} \approx \eta(1 - E_{ai}/E_{in})^{-1}, \quad (31)$$

TABLE 2.

$\mu$	$\omega_0 = 1, \tau_a = 0.1$		$\omega_0 = 1, \tau_a = 10$		$\omega_0 = 10, \tau_a = 0.01$	
	$\eta$	$E_{ai}/E_{in}$	$\eta$	$E_{ai}/E_{in}$	$\eta$	$E_{ai}/E_{in}$
0.1	0.189	0.178	0.190	0.176	0.194	0.089
0.2	0.249	0.172	0.236	0.163	0.257	0.085
0.5	0.286	0.163	0.260	0.145	0.295	0.077
1.0	0.275	0.164	0.234	0.136	0.265	0.069

where  $E_{at}$  is the absorber internal energy by the time equation (30) is used (see table 2). With this correction in mind, we conclude that (i) the numerical simulations confirm equations (16) and (29) (but not equation (27)), and (ii) the errors of each of the two expressions (16) and (29) are about the same magnitude as the scatter in numerically obtained values of  $\eta_{pl}(\mu)$ . In summary, *the hydrodynamic efficiency of shells illuminated by ion beams—when a significant fraction of the shell mass is being heated simultaneously—must be calculated within the framework of nonsteady hydrodynamics.*

#### 4. Spherical shells

In the spherical case the path length of the pusher is limited by its initial radius  $r_p$ , condition (12) in general cannot be satisfied, and we must revise the definition (2) of the HE. Since the stage of pusher acceleration in spherical geometry is followed by the cumulation stage at which the pusher kinetic energy is converted into the compression energy of the pusher itself and that of the central gas, the spherical HE can be defined as

$$\eta_{sp} = \frac{E_p + E_c}{E_{in}} \Big|_{u_a = 0}, \quad (32)$$

where  $E_p$  and  $E_c$  are the total energies of the pusher and the central gas by the time of maximum compression when the velocity  $u_a$  of the pusher-absorber interface drops to zero.

With addition of a new dimensional parameter  $R$ , the spherical HE becomes a function of three “external” dimensionless parameters:

$$\eta_{sp} = \eta_{sp}(\mu, \delta, \tau_{in}), \quad (33)$$

$$\mu = \frac{M_p}{M_a}, \quad \delta = \frac{R - r_a}{R}, \quad \tau_{in} = \frac{t_{in}}{R} \sqrt{\frac{E_{in}}{M_a}}. \quad (34)$$

In the plane-parallel limit,  $\delta = \tau_{in} = 0$  and

$$\eta_{pl}(\mu) = \eta_{sp}(\mu, 0, 0). \quad (35)$$

In spherical geometry—as contrasted to the plane-parallel one—it is much more difficult to construct a simple analytical model that would reveal (quantitatively as well as qualitatively) the functional form of equation (33). In table 3 the values of  $\eta_{sp}(\mu, \delta, \tau_{in})$  as obtained from 1D hydrodynamic code calculations are presented. In all the runs included in table 3 the pusher and absorber were of gold (initial density  $\rho_{0a} = \rho_{0p} = 19.5$  g/cc), the central gas (deuterium) comprised 0.5% of the pusher mass, and the initial shell radius and specific energy input were  $R = 1$  mm,  $E_{in}/M_a = 10$  MJ/g. A salient feature of the functional dependence of  $\eta_{sp}$  on parameters  $\delta$  and  $\tau_{in}$ , clearly illustrated by table 3, is that for any fixed  $\mu$  the values of  $\eta_{sp}(\mu, \delta, \tau_{in})$  monotonously decrease with increasing  $\delta$  and  $\tau_{in}$ —the fact that can actually be inferred from the most general properties of spherical flows. The latter means that *from the point of view of the HE theory the lesser the values of dimensionless parameters  $\delta$  and  $\tau_{in}$ , the more efficient is an ICF target.* It should be noted also that with increasing  $\delta$ ,  $\tau_{in} > 0$  the maximum of  $\eta_{sp}$  over  $\mu$  shifts to smaller values of the latter, namely to  $\mu = 0.2 - 0.4$ .

To check the weak dependence of  $\eta_{sp}$  on parameters other than  $\mu$ ,  $\delta$ , and  $\tau_{in}$ , a series of runs have been performed in which for  $\delta = \tau_{in} = 0.1$ ,  $\mu = 0.1, 0.2, 0.5, 1.0$  different combinations of the values  $E_{in}/M_a = 1, 10$  MJ/g,  $R = 1, 10$  mm were probed, and a beryllium absorber instead of the gold was tried. The values of the HE obtained in these runs differ from those given in table 3 by no more than 8%.

TABLE 3. Hydrodynamic efficiency  $\eta_{sp}(\mu, \delta, \tau_{in})$  of spherical shells

$\tau_{in}$	$\delta$	$\mu$					
		0.05	0.1	0.2	0.333	0.5	1.0
0.0316	0.0316	0.144	0.196	0.241	0.256	0.257	0.231
	0.1	0.112	0.157	0.195	0.207	0.204	0.181
	0.316	0.058	0.083	0.100	0.098	—	—
0.1	0.0316	0.135	0.179	0.217	0.230	0.226	0.201
	0.1	0.111	0.152	0.186	0.196	0.193	0.171
	0.316	0.058	0.081	0.098	0.095	—	—
0.316	0.0316	0.106	0.141	0.170	0.181	0.178	0.155
	0.1	0.095	0.128	0.155	0.163	0.158	0.138
	0.316	0.054	0.075	0.088	0.086	—	—
1.0	0.0316	0.059	0.082	0.104	0.114	0.116	0.105
	0.1	0.056	0.078	0.098	0.105	0.103	0.089
	0.316	0.035	0.052	0.062	0.059	—	—

### 5. Nonhomogeneous absorbers

The above results were obtained under the assumption that absorber is homogeneous in the initial composition and has a uniform distribution of the energy deposition rate. Obviously, higher values of the HE can be achieved with nonhomogeneous absorbers, when a hot low-density plasma layer is created near the pusher-absorber interface. On the one hand, such a nonhomogeneity is a natural consequence of the increase in the stopping power by the end of the range of charged particles. On the other hand, it may be enhanced with a two-layer absorber composed of a low-Z (Li, Be, . . .) internal and a high-Z (Au, Pb, . . .) external layer; in this case the internal layer will have a lower initial density and a higher energy deposition rate per unit mass.

In planar geometry the effect of a nonhomogeneous absorber structure can be investigated in the framework of the stepwise-density-profile approximation. Let  $M_{a1} = (1 - \nu)M_a$ ,  $\rho_{a1}(t)$  and  $M_{a2} = \nu M_a$ , and  $\rho_{a2}(t) = \omega \rho_{a1}(t)$  be the masses and densities of, respectively, the internal and external absorber layers (more dense external layer is often called tamper), where  $0 < \nu < 1$  and  $\omega > 1$  are constants. Assuming that the pusher of mass  $M_p = \mu M_a$  is infinitely thin and having performed the calculations analogous to those presented in section 3, we arrive at the following expression for the plane-parallel HE:

$$\eta_{pl} = \left[ 1 + (1 - \Lambda) \left( \frac{2}{3} + \frac{1}{3\mu} \right) + (4 - \Lambda) \frac{\mu}{3} \right]^{-1}, \quad (36)$$

where

$$\Lambda = 4(\omega - 1) \left( \omega + \frac{\nu}{1 - \nu} \right) \left( \omega \frac{1 + \nu}{\nu} + \frac{\nu}{1 - \nu} \right)^{-2}. \quad (37)$$

As a first example of how to make use of equations (36) and (37), consider a nonuniform heating of initially homogeneous absorber. If one takes the stopping power to be inversely proportional to the ion energy (Ahlen 1980; the extreme case of a nonuniform energy deposition by stopping of fast charged particles), then half of the beam energy will be released over the last quarter of the range. The latter means that in our model we must take  $\omega =$

3,  $\nu = 0.75$  — which infers  $\Lambda = 0.48$ . For a fixed  $\Lambda$  the function  $\eta_{pl}(\Lambda, \mu)$  achieves maximum at

$$\mu_{\max} = \sqrt{\frac{1 - \Lambda}{4 - \Lambda}}, \quad (38)$$

which, in our case, amounts to  $\eta_{\max} = 0.445$  and exceeds the maximum of  $\eta_{pl}(\mu)$  from equation (16) by 33%. A corresponding code run with the energy release rate  $q \sim (m_a - m)^{-1/2}$ , where  $m$  is the mass coordinate, showed an excellent agreement with this estimate. In practice, however, the gain in HE due to the stopping power growth by the end of the range is always below 30% for the reasons pointed out in section 1.

Equations (36) and (37) also provide a ready solution to the following problem: to find the optimum tamper mass  $\nu = \nu_{\max}$  for a given density ratio  $\omega$  between the two absorber layers. According to equation (36), for any fixed  $\mu$  the maximum of  $\eta_{pl}$  coincides with the maximum of  $\Lambda(\nu, \omega)$  attained at  $\nu = \nu_{\max}$ , where

$$\frac{\nu_{\max}}{1 - \nu_{\max}} = [\omega^2 + \sqrt{\omega^3(\omega - 1)}]^{1/3} + [\omega^2 - \sqrt{\omega^3(\omega - 1)}]^{1/3}. \quad (39)$$

Table 4 shows the values of  $\nu_{\max}$ ,  $\mu_{\max}$ , and  $\eta_{\max}$  representing the maxima of  $\eta_{pl}$  over two parameters  $\nu$  and  $\mu$  for different values of  $\omega$ .

In spherical geometry, unfortunately, the increase in the HE values illustrated in table 4 cannot be fully realized. The fact is that, when we replace part of the high-density absorber with a low-density layer (retaining either the total mass or the optical depth for beam ions), we are usually forced to degrade its dynamic quality characterized by parameters  $\delta$  and  $\tau_{in}$  (34). As an example, consider a modification of the gold shell from table 3 with  $\delta = \tau_{in} = 0.1$  in which the internal half of the absorber has been replaced by a beryllium layer of five times lower mass but with a fivefold increase in the mass heating rate. The relative tamper mass  $\nu = 0.833$  turns out to be close to the optimum one for  $\omega = 10 = \rho_{Au}/\rho_{Be}$  (see table 4). After such a modification the dimensionless parameters  $\delta, \tau_{in}$  become  $\delta = 0.173$ ,  $\tau_{in} = 0.129$ . The HE values obtained for a shell thus modified are given in table 5. Having compared them with those given in table 3, one sees that a substantial ( $\geq 60\%$ ) increment in  $\eta_{sp}$  values can be achieved for small  $\mu \leq 0.1$  only, while the maximum value of HE has increased by a mere 35%.

TABLE 4.

$\omega$	2	3	6	10	40
$\nu_{\max}$	0.747	0.815	0.848	0.883	0.946
$\mu_{\max}$	0.425	0.354	0.317	0.273	0.179
$\eta_{\max}$	0.404	0.477	0.519	0.571	0.697

TABLE 5.

$\mu$	0.1	0.2	0.5	1.0
$\eta_{sp}$	0.247	0.260	0.219	0.172

## 6. Conclusions

The analysis performed in this paper clearly demonstrates that the hydrodynamic efficiency of shells illuminated by charged particle beams must be evaluated under nonsteady approximations. In contrast to steady-state models, the nonsteady HE turns out to be insensitive to the details of the equation of state.

The HE  $\eta_{pl}$  of homogeneous planar shells essentially depends on one dimensionless parameter  $\mu$  — the pusher/absorber mass ratio; this dependence is satisfactorily reproduced by a simple formula (16).

The HE  $\eta_{sp}$  of homogeneous spherical shells essentially depends on three dimensionless parameters:  $\mu$ , the pusher/absorber mass ratio;  $\delta$ , the inverse of the absorber aspect ratio; and  $\tau_{in}$ , the dimensionless time of illumination (see equation (34)). Function  $\eta_{sp}(\mu, \delta, \tau_{in})$  has a maximum along  $\mu$ -axis at  $\mu = \mu_{max} \approx 0.2-0.5$  and monotonously decreases with increasing  $\delta > 0$ ,  $\tau_{in} > 0$ .

A nonhomogeneous absorber with a hot low-density inner edge has an advantage over the homogeneous one, but in practice a substantial ( $\approx 50\%$ ) gain in the HE efficiency through this effect can be achieved only for low enough pusher masses,  $\mu \lesssim 0.1$ .

## REFERENCES

- AFANAS'EV, YU. V., GAMALII, E. G., KROKHIN, O. N. & ROZANOV, V. B. 1975 *Prikl. Mat. Mekh. (Soviet Appl. Math. Mech.)*, **39**, 451.
- AFANAS'EV, YU. V., ISAKOV, V. A. & KROKHIN, O. N. 1981. *Zh. Eksp. Teor. Fiz. (Soviet Phys. JETP)*, **81**, 1714.
- AFANAS'EV, YU. V., GAMALII, E. G., GUS'KOV, S. YU. & ROZANOV, V. B. 1982 In: Theory of Heating and Compression of Low-Entropy Thermonuclear Targets (in Russian), Trudy FIAN (Proc. Lebedev Phys. Inst., Academy of Sci. USSR), **134**, 52.
- AHLEN, S. P. 1980 *Rev. Mod. Phys.*, **52**, 121.
- BASKO, M. M. 1984 *Fiz. Plazmy (Soviet J. Plasma Phys.)*, **10**, 1195.
- BASKO, M. M. 1985 *Teplofiz. Vys. Temp. (Soviet High Temper.)*, **23**, 483.
- BASKO, M. M. & SOKOLOVSKII, M. V. 1982 *Fiz. Plazmy (Soviet J. Plasma Phys.)*, **8**, 519.
- DUDERSTADT, J. J. & MOSES, G. A. 1982 *Inertial Confinement Fusion*. (John Wiley & Sons, New York).
- MAX, C. E., LINDL, J. D. & MEAD, W. C. 1983 *Nucl. Fusion*, **23**, 131.
- NEMCHINOV, I. V. 1961 *Prikl. Mekh. Tekhn. Fiz. (Soviet Appl. Mech. Techn. Physics)*, **1**, 17.
- SEDOV, L. I. 1981 *Similarity and Dimensionality Methods in Mechanics* (in Russian) (Nauka, Moscow), Chap. IV, §15.
- ZEL'DOVICH, YA. B. & RAIZER, YU. P. 1966 *Physics of Shock Waves and High-Temperature Hydrodynamic Phenomena*. (Academic Press, New York and Nauka, Moscow), Vol. I, Chap. IV.